

# Static Recrystallization Modelling of Hot Deformed Microalloyed Steels at Temperatures below the Critical Temperature

S. F. MEDINA and J. E. MANCILLA<sup>1)</sup>

Centro Nacional de Investigaciones Metalúrgicas, CSIC, Av. Gregorio del Amo 8, 28040-Madrid, Spain.

1) Centro de Investigación en Materiales Avanzados, León Tolstoi 166, 31109-Chihuahua, México.

(Received on December 4, 1995; accepted in final form on April 12, 1996)

Using torsion tests and applying the back extrapolation method a model has been constructed to predict the recrystallized fraction of deformed austenite in Nb, V and Ti microalloyed steels at temperatures below the temperature at which the inhibition of recrystallization commences due to induced precipitation. This temperature, named static recrystallization critical temperature, is modelled as a function of grain size, strain and the solubility temperature. A discussion is made of the importance of being able to predict SRCT in order to effectively apply the model of static recrystallization at temperatures both above and below it. It is demonstrated that Niobium precipitates delay the recrystallization most.

KEY WORDS: static recrystallization; modelling; microalloyed steels; static recrystallization critical temperature (SRCT).

## 1. Introduction

When austenite in microalloyed steels is deformed, it is known that strain induced precipitation inhibits static recrystallization and if the strain is applied at temperatures lower than that at which this inhibition commences, a temperature which we shall henceforth refer to as the static recrystallization critical temperature (SRCT), the recrystallization kinetics are different, where the activation energy for the recrystallization stops being a constant and comes to be a function of the temperature.<sup>1,2)</sup> Most models for static recrystallization in microalloyed steels do not make provision for this and are applied only in the range of temperatures where the microalloy is in solution or where precipitation has still not been sufficient to inhibit recrystallization. Some authors<sup>3-6)</sup> establish for Nb microalloyed steels that when the strain temperature is lower than the solubility temperature of the precipitates (carbonitrides of Nb) recrystallization is more difficult and the activation energy increases slightly. Recent studies, however, have shown that the activation energy varies significantly when temperatures are below SRCT and this variation may be expressed using an Arrhenius-type law.<sup>7-9)</sup>

The temperature defined above as SRCT is approximately the same as  $T_{nr}$  defined by Jonas *et al.*<sup>10-14)</sup> as the two refer to the start of the inhibition of recrystallization, though the methods for their determination are different.<sup>9)</sup> However, there are certain differences between both magnitudes which will be discussed later on.

Knowing the SRCT of microalloyed steels is of great importance in hot rolling,<sup>1,10-12)</sup> as a rolling whose final

passes take place at temperatures below SRCT will give rise to an accumulated strain of the austenite. The consequence of this will be that the ferrite grain which is obtained after the  $\gamma \rightarrow \alpha$  transformation will be much smaller than if the successive passes are carried out at temperatures above SRCT.<sup>1)</sup>

In this work the static recrystallization kinetics of eight microalloyed steels with Nb, V or Ti are studied using torsion tests. An expression is given to predict the variation in the activation energy when the temperature is lower than SRCT. In this way the recrystallization kinetics are modelled at temperatures in the austenite phase below SRCT.

## 2. Materials and Experimental Procedure

The microalloyed steels used in this study are the same as those used to determine the activation energy<sup>15)</sup> and to model the static recrystallization kinetics<sup>16)</sup> when all the elements are in solution. A total of eight steels are studied: three Ti steels, three V steels and two Nb steels. The content of the microalloying element (V, Ti, Nb) varied from one steel to another within the compositions typical of hot rolled steels. The chemical composition of steels used are shown in **Table 1**, together with the cooling critical temperature ( $Ar_3$ ), and the austenite grain size ( $D$ ) at reheating temperature ( $1230^\circ\text{C} \times 10 \text{ min}$ ). The recrystallized fraction was determined using the "back extrapolation" method.<sup>17)</sup>

The torsion tests were carried out using a wide range of temperatures in order to be able to determine with precision the SRCT of each one. The testing conditions have been described elsewhere.<sup>15)</sup>

**Table 1.** Chemical composition (wt%) of microalloyed steel used, cooling critical temperatures ( $Ar_3$ , at  $0.2^\circ\text{C}/\text{s}$ ) and austenite grain size ( $D$ ,  $\mu\text{m}$ ) at  $1230^\circ\text{C} \times 10$  min; being  $X_i = \text{Mo}, \text{Ti}, \text{V}, \text{Nb}$ .

Steel	C	Si	Mn	$X_i$	N	$Ar_3, ^\circ\text{C}$	$D, \mu\text{m}$
T5	0.15	0.24	1.12	Ti=0.021	0.0105	791	29
T2	0.15	0.27	1.25	Ti=0.055	0.0100	774	95
T3	0.15	0.26	1.10	Ti=0.075	0.0102	779	90
V1	0.11	0.24	1.10	V=0.043	0.0105	786	172
V2	0.12	0.24	1.10	V=0.060	0.0123	782	167
V3	0.11	0.24	1.00	V=0.093	0.0144	784	165
N1	0.11	0.24	1.23	Nb=0.041	0.0112	786	122
N2	0.11	0.24	1.32	Nb=0.093	0.0119	786	116

### 3. Results

The form of the recrystallized fraction against time curves were similar for all the microalloyed steels, *i.e.* the curves presented a plateau when the temperature was lower than SRCT. The plateau is caused by strain induced precipitation. By way of example, **Fig. 1** shows the recrystallized fraction for steel N2 at a strain of 0.20, strain rate of  $3.63 \text{ s}^{-1}$  and several temperatures, with a plateau appearing on the curve corresponding to  $1025^\circ\text{C}$ . In the same way, **Fig. 2** shows the recrystallized fraction for steel V3, at a strain of 0.35, it being observed that the plateau starts to appear on the curve corresponding to  $950^\circ\text{C}$ . In Ti microalloyed steels a plateau is presented as a consequence of the strain induced precipitation of the Ti which is still dissolved at the reheating temperature ( $1230^\circ\text{C} \times 10$  min). It should be noted that at the above temperature, Ti is partially precipitated, the quantities dissolved in the austenite being 0.022, 0.041 and 0.002 (wt%) for steels T2, T3 and T5, respectively.<sup>18,19</sup> **Figure 3** corresponds to steel T2, where the plateau starts to appear on the curve corresponding to  $900^\circ\text{C}$ .

The values of  $t_{0.5}$  and  $n$  were determined for each temperature and strain. Reference 15) presents the values of  $t_{0.5}$  for all the microalloyed steels at the testing temperatures, and of  $n$  for temperatures where the recrystallized fraction against time curve did not show a plateau, *i.e.* where the recrystallization kinetics were not interrupted by induced precipitation.

Recrystallized fraction curves were also determined for steel V3 with a different initial grain size, specifically  $125 \mu\text{m}$ , obtained by reheating at  $1100^\circ\text{C} \times 10$  min. The values of  $t_{0.5}$  and  $n$  obtained are also presented in Ref. 15) and, as will be seen later, and allow us to estimate the influence of grain size on the value of SRCT.

### 4. Discussion and Modelling

In the recrystallized fraction against time curves for the microalloyed steels, the start and finish of each plateau coincide approximately with the start and finish of induced precipitation and it is in the limited period of time between these two points where the recrystallization-precipitation interaction takes place. Nevertheless, before the start and after the finish of precipitation the recrystallized fraction obeys the first ap-

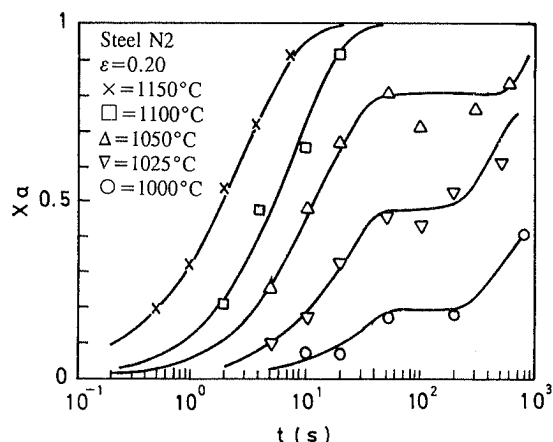


**Fig. 1.** Recrystallized fraction ( $X_a$ ) plotted against time. Steel N2;  $\varepsilon = 0.20$ ;  $\dot{\varepsilon} = 3.63 \text{ s}^{-1}$ .

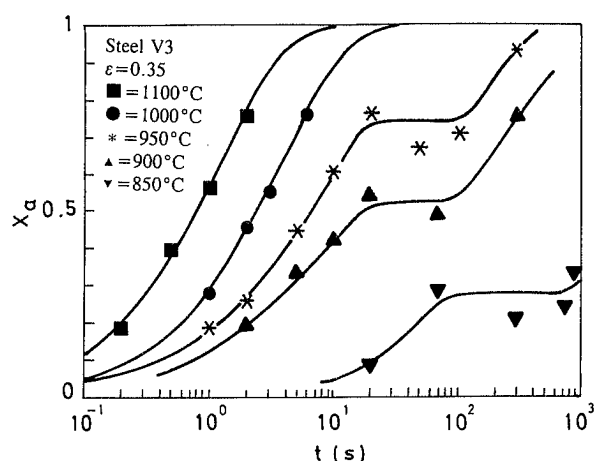


**Fig. 2.** Recrystallized fraction ( $X_a$ ) plotted against time. Steel V3;  $\varepsilon = 0.35$ ;  $\dot{\varepsilon} = 3.63 \text{ s}^{-1}$ .

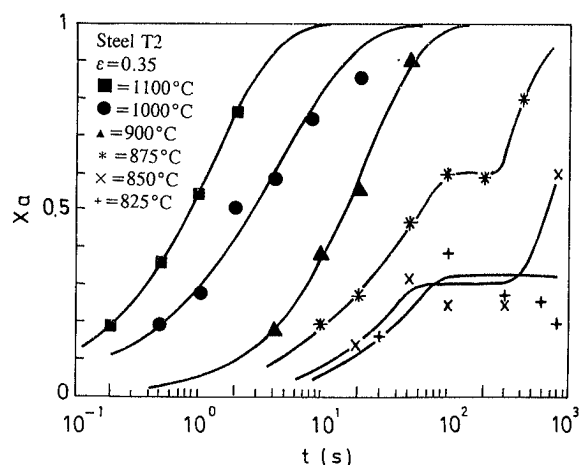


**Fig. 3.** Recrystallized fraction ( $X_a$ ) plotted against time. Steel T2;  $\varepsilon = 0.35$ ;  $\dot{\varepsilon} = 3.63 \text{ s}^{-1}$ .

proximation to Avrami's law.

According to the general equation for the parameters  $t_{0.5}$ ,<sup>15,16</sup> the activation energy ( $Q$ ) was measured taking  $\ln(t_{0.5})$  as a function of  $1/T$ , the slope being equal to  $Q/R$ . The graphic representation for the microalloyed steels show two different parts (**Fig. 4**). The first part is a straight line and the second is curvilinear, with the activation energy ceasing to be a constant and coming

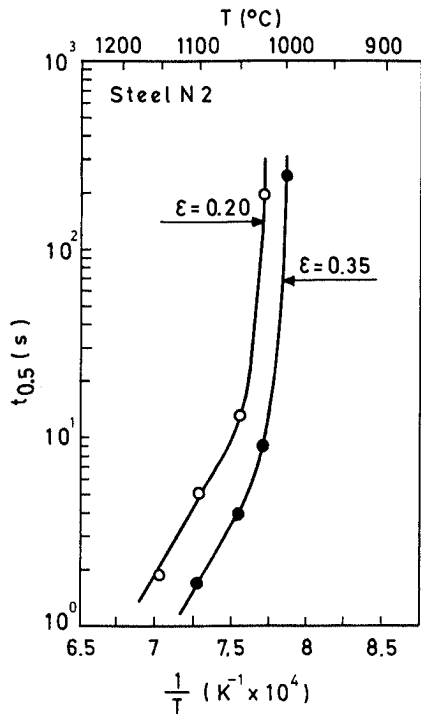


Fig. 4. Plot of  $t_{0.5}$  against the reciprocal of the absolute temperature. Steel N2.

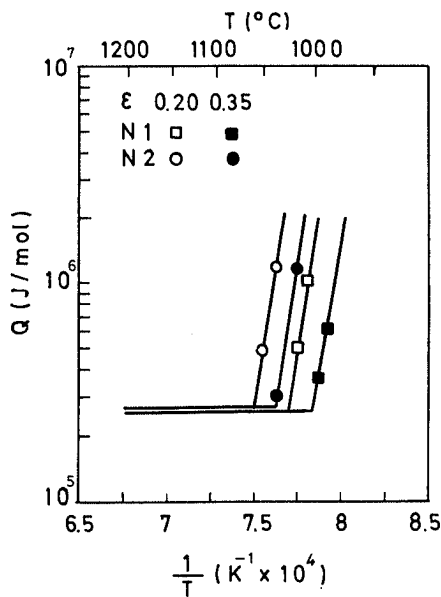


Fig. 5. Plot of the activation energy against the reciprocal temperature for steel N2.

to be a function of the temperature. The point at which activation energy becomes a function of the temperature, in other words SRCT, indicates the start temperature of induced precipitation and this point may be determined with complete precision if the activation energy is represented against the inverse of the temperature, as in Fig. 5. The intersection of the horizontal line ( $Q$  constant) with the sloping line gives the value of SRCT, it being observed that its value drops as the strain increases. Figure 6 also shows the representation of  $t_{0.5}$  against  $1/T$  for steel V3, where once again the influence of the strain and of the grain size can be seen. A reduction in the grain size also reduces the value of SRCT.

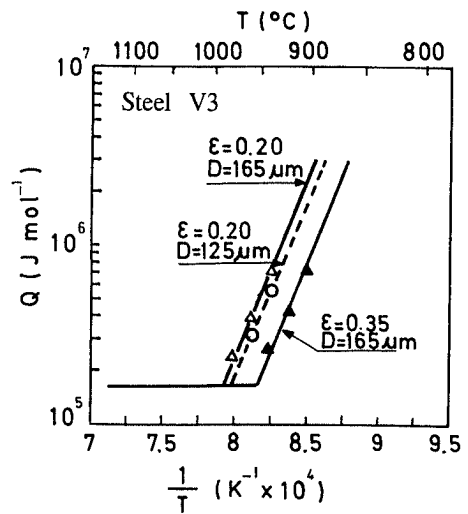


Fig. 6. Plot of the activation energy against the reciprocal temperature for steel V3.

Table 2. Static recrystallization critical temperature (SRCT) for the steels used.

Steel	SRCT (K)	
	$\epsilon=0.20$	$\epsilon=0.35$
T2	1181	1170
T3	1230	1215
T5	1117	1105
V1	1176	1153
V2	1198	1180
V3	1262* 1254**	1227*
N1	1303	1278
N2	1333	1313

\* austenite grain size = 165  $\mu\text{m}$   
 \*\* austenite grain size = 125  $\mu\text{m}$

The determination of SRCT in microalloyed steels is important as its value indicates the maximum temperature for the application of this model. At the same time SRCT indicates the starting temperature of induced precipitation and the loss of constancy of  $Q$  which becomes a function of the temperature. The values of SRCT for all the microalloyed steels were determined using the method indicated in Figs. 5 and 6. The values found (Table 2) indicate that SRCT is a function of strain, grain size and obviously of the chemical composition. In order to model SRCT an expression of the following type was selected:

$$\text{SRCT} = M - KD^{\alpha} \epsilon^{\beta} \dots\dots\dots(1)$$

where  $M$  is a temperature close to the solubility temperature of the precipitate. The equations encountered are the following:

a) Vanadium steels (V1, V2 and V3):

$$\text{SRCT(K)} = T_s - 1.05 \times 10^3 D^{-0.35} \epsilon^{0.50} \dots\dots\dots(2)$$

$T_s$  represents the solubility temperature of VN in the steels V1, V2 and V3, respectively, determined using the equation:  $\log(V)(N) = -8700/T + 3.63 \dots$  (Ref. 20)).

b) Niobium steels (N1 and N2):

$$SRCT(K) = T_s - 1.05 \times 10^3 D^{-0.35} \epsilon^\beta \dots\dots\dots(3)$$

Equation (3) is applicable to steel N1 where  $\beta=0.5$  and  $T_s$  is the solubility temperature of NbN, determined using the equation:  $\log(Nb)(N) = -8500/T + 2.80 \dots$  (Ref. 20)).

Steel N2 shows an Nb/N relation (wt%) greater than the stoichiometric relation of NbN and given that the temperature  $T_s$  of these is similar to those of NbC it seems that the inhibition of recrystallization is due in part to the latter. Therefore, Eq. (3) is applicable to steel N2 where  $\beta=0.28$  and  $T_s$  is the solubility temperature of NbC, determined using equation:  $\log(Nb)(C) = -7900/T + 3.42 \dots$  (Ref. 20)).

c) Titanium steels (T2, T3 and T5):

$$SRCT(K) = T_s - 1.05 \times 10^3 D^{-0.35} \epsilon^\beta \dots\dots\dots(4)$$

Equation (4) is applicable to steels T2 and T3 where  $\beta=0.20$  and  $T_s$  is the solubility temperature of TiC, in accordance with the equation:  $\log(Ti)(C) = 10475/T + 5.33 \dots$  (Ref. 20)). The Ti contents considered are those in solution at 1230°C, i.e. 0.022 (wt%) for T2 and 0.041 (wt%) for T3.

In the case of steel T5, and Ti/N relation (wt%) is lower than the stoichiometric relation of TiN and therefore the Ti dissolved at 1230°C (0.002 wt%) may form Titanium nitrides or carbonitrides during induced precipitation. Equation (4) is applicable to steel T5 making  $\beta=0.20$  and  $T_s$  would be a hypothetical solubility temperature of a carbonitride compound of titanium, whose value would be approximately 1360 K.

These results show that the exponent of the strain could indicate the nature of the precipitates. Thus, when the precipitates are clearly nitrides or when these are preponderant, the exponent is approximately equal to 0.5. However, when the precipitates are carbides, or these are preponderant over the nitrides, the exponent is less than 0.5, giving values close to 0.2. The difference between  $T_s$  and SRCT is greater with a strain involving carbides than for the same strain involving nitrides. But a variation in the strain causes the SRCT to decrease more in the case of nitrides than with carbides.

Figure 7 shows the values of SRCT predicted by the previous equations against the experimental values, obtaining an index of correlation of 0.996.

On the other hand, SRCT coincides approximately with the no recrystallization temperature ( $T_{nr}$ ) when this is determined with interpass times of approximately 30 s or more,<sup>9)</sup> as in this case  $T_{nr}$  also coincides with the starting temperature of induced precipitation. When the interpass times fixed to determine  $T_{nr}$  are small this magnitude fixes the temperature below which a hardening of the austenite starts to be detected due to the fact that the interpass time is insufficient for it to totally recrystallize, though induced precipitation has still not taken place. However, SRCT will always be the temperature at which the induced precipitation commences as it is independent of the time.

It has been seen before that when the temperature is

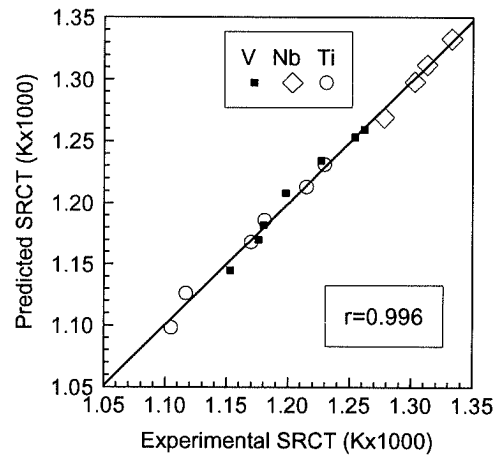


Fig. 7. Predicted against experimental SRCT values.

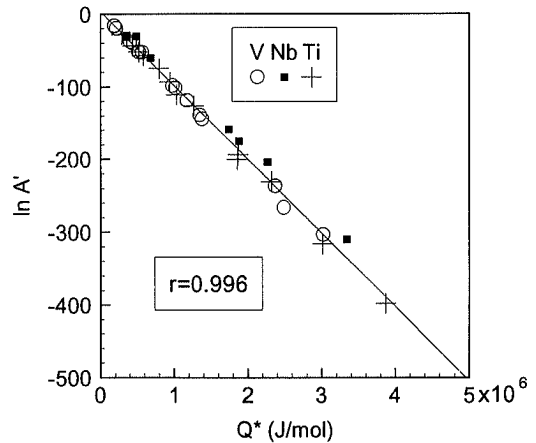


Fig. 8. Coefficient A' in Eq. (6) against the activation energy ( $Q^*$ ).

below SRCT the activation energy of microalloyed steels is a function of the temperature. From Figs. 5 and 6 it is possible to deduce the type of expression for the activation energy when  $T < SRCT$ :

$$Q^* (J mol^{-1}) = Q \exp \frac{H}{R} \left( \frac{1}{T} - \frac{1}{SRCT} \right) \dots\dots\dots(5)$$

where  $H$  represents a pseudo-energy,  $Q$  is the activation energy when the elements are in solution<sup>15)</sup> and SRCT is given by the equations in the appendix. The value of  $H$  was different for each family of steels, finding values of 875 000 J mol<sup>-1</sup>, 500 000 J mol<sup>-1</sup> and 400 000 J mol<sup>-1</sup> for the Nb, Ti and V steels, respectively. These values may indicate the relative efficiency of the different types of precipitates in inhibiting recrystallization.

On the other hand, Eq. (5) shows that SRCT represents the start temperature below which the activation energy begins to increase. Bearing in mind that SRCT is a function not only of the content and nature of the microalloys but also of the strain and of the grain size, a simple function for  $t_{0.5}$  was found:

$$t_{0.5} = A' \exp \frac{Q^*}{RT} \dots\dots\dots(6)$$

It was also found that  $A'$  is related with  $Q^*$ . The values of  $A'$ , calculated in accordance with Eq. (6), were represented against the values of  $Q^*$  (Fig. 8), having

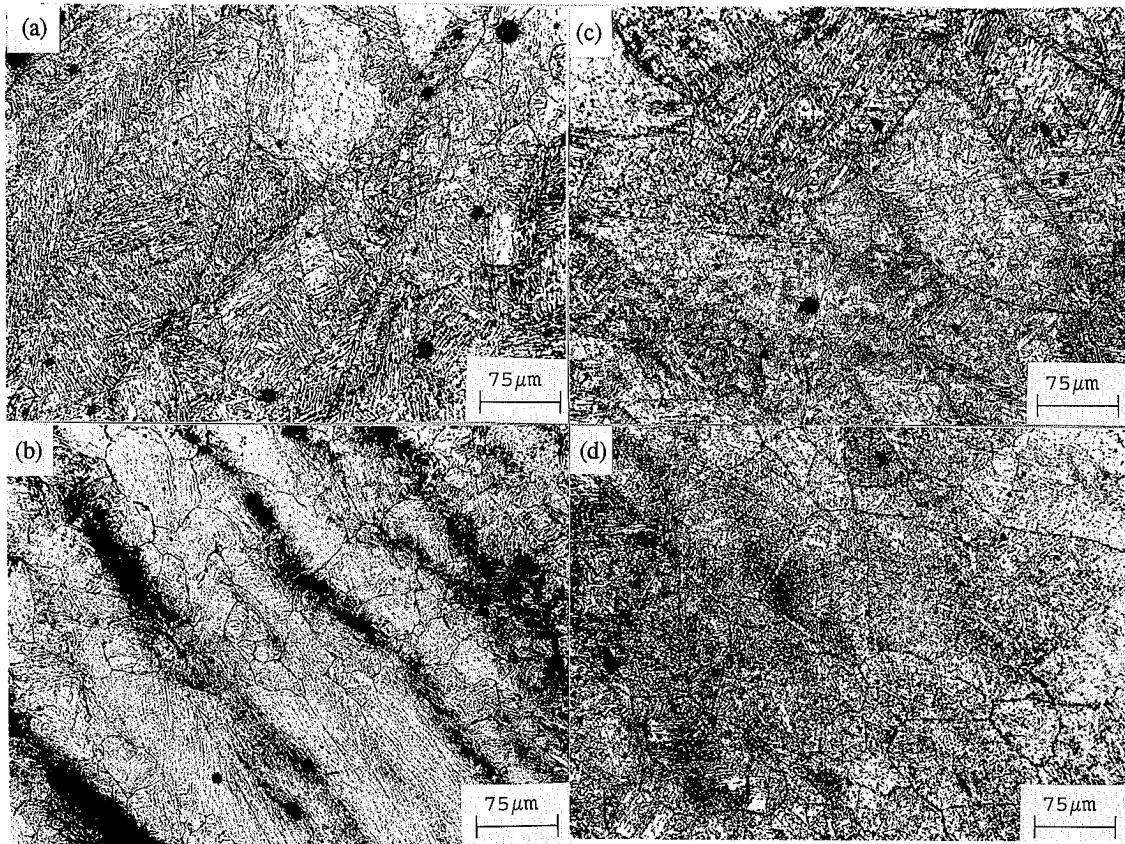


**Fig. 9.** Microstructures of recrystallized fraction in austenite strained at different temperatures and recrystallization times ( $t$ ) for the steel V3. ( $\dot{\epsilon} = 3.63 \text{ s}^{-1}$ );  $X_{am}$  = measured recrystallized fraction;  $X_{ac}$  = calculated recrystallized fraction)

(a)  $\epsilon = 0.35$ ;  $T = 1\,000^\circ\text{C}$ ;  $t = 2 \text{ s}$ ;  $X_{am} = 0.07$ ;  $X_{ac} = 0.02$   
 (b)  $\epsilon = 0.35$ ;  $T = 1\,000^\circ\text{C}$ ;  $t = 70 \text{ s}$ ;  $X_{am} = 0.45$ ;  $X_{ac} = 0.42$   
 (c)  $\epsilon = 0.20$ ;  $T = 1\,000^\circ\text{C}$ ;  $t = 10 \text{ s}$ ;  $X_{am} = 0.05$ ;  $X_{ac} = 0.03$   
 (d)  $\epsilon = 0.20$ ;  $T = 1\,000^\circ\text{C}$ ;  $t = 200 \text{ s}$ ;  $X_{am} = 0.35$ ;  $X_{ac} = 0.31$

obtained an index of correlation between both magnitudes of 0.996, as can easily be verified. The expression for the relation found was:

$$A' = 25.3318 \exp(-1.0147 \times 10^{-4} Q^*) \dots\dots\dots(7)$$

Finally, for exponent  $n$  of the Avrami equation, the expression taken is that which corresponds to equations referring to the same steels when the elements are in solution.<sup>16)</sup> However, these expressions do not take into account the presence of the plateau and only represent the tendency of  $n$  to diminish with the temperature. Therefore, the value of  $n$  represents an estimation of a hypothetical mean value which would correspond to a curve of the recrystallized fraction crossing the plateau at its halfway point and a slope equal to that of the curve before and after the presence of the plateau.

The inhibition of recrystallization due to the presence of precipitated particles was studied by Zener,<sup>21)</sup> who established that a grain boundary acting as recrystallization front can be subjected to a retarding force due to precipitated stable particles. The retarding force is directly proportional to the volume fraction of particles and to the surface energy of the boundary and inversely proportional to the radius of the supposedly spherical particle. Ashby *et al.*<sup>21)</sup> revised Zener's

calculation so that it accounts for aspects of the nature of the interface and the particle by considering boundaries that by-pass or pass through particles. Accordingly, the authors consider that the value of  $H$ , which is different for each type of microalloyed steel, may be related with the size of the precipitates, as has been indicated above.

In order to verify and illustrate the model, observations were made of some microstructures obtained by quenching, showing the fraction of the austenite recrystallized at temperatures below SRCT. Due to their low carbon content, the steels studied were of low hardenability. Nevertheless, some completely martensitic microstructures were obtained, which were subsequently attacked in a saturated solution of picric acid in order to observe the austenite grain boundaries. By way of example, Figs. 9(a) to 9(d) show the austenite microstructures of steel V3 obtained at a reheating temperature of  $1\,230^\circ\text{C} \times 10 \text{ min}$ , strains of 0.35 (a, b) and 0.20 (c, d) at  $900^\circ\text{C}$  and holding times of 2 s (a), 70 s (b), 10 s (c) and 200 s (d), and immediately quenched by a flow of water. **Figures 10(a) and 10(b)** show the microstructures corresponding to steel V2, obtained at a reheating temperature of  $1\,230^\circ\text{C} \times 10 \text{ min}$ , strains of 0.35 at  $875^\circ\text{C}$  and held at this temperature for 5 and 10 sec, respectively, followed by quenching. A note at the

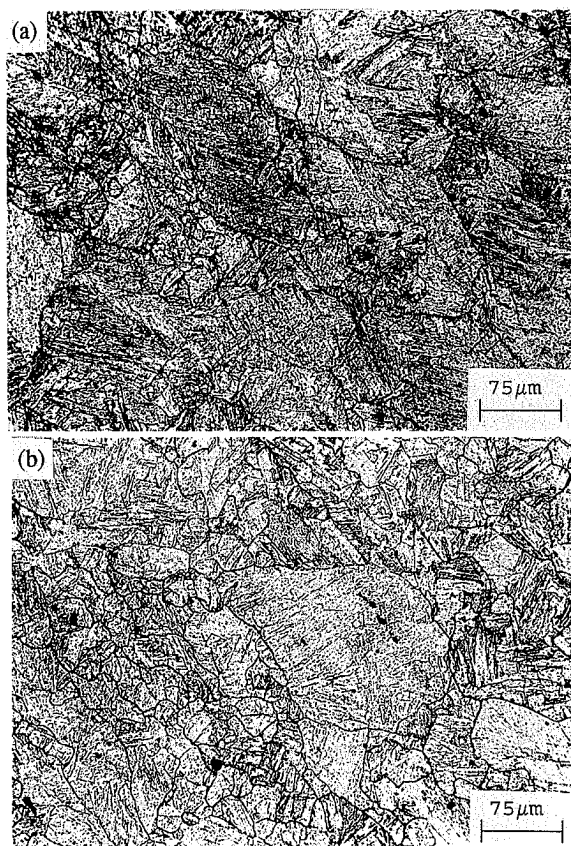


**Fig. 10.** Microstructures of recrystallized fraction in austenite strained at different temperatures and recrystallization times ( $t$ ) for the steel V2. ( $\dot{\epsilon}=3.63\text{ s}^{-1}$ );  $X_{am}$ =measured recrystallized fraction;  $X_{ac}$ =calculated recrystallized fraction)  
 (a)  $T=875^{\circ}\text{C}$ ;  $t=5\text{ s}$ ;  $X_{am}=0.12$ ;  $X_{ac}=0.03$   
 (b)  $T=875^{\circ}\text{C}$ ;  $t=100\text{ s}$ ;  $X_{am}=0.50$ ;  $X_{ac}=0.37$

foot of the figures indicates the recrystallized fraction determined experimentally by means of the observation of several fields using optical microscopy, the results being verified by the recrystallized fraction against time curves. The recrystallized fraction predicted by the model is also indicated. The equations used and the data obtained from the calculations of the recrystallized fraction are shown in the appendix. The good prediction of the model can be seen, though it should be noted that in general this precision depends to a great extent on the content of the precipitate forming elements, in other words the nature of the precipitates. In the case of V microalloyed steels the precipitates are always nitrides (VN), even for high carbon contents, and Eq. (2) gives good exactitude for SRCT. In the case of the Nb microalloyed steels, if they have a very low carbon content ( $<0.1\text{ wt}\%$ ) the precipitates are preponderantly nitrides, but if the carbon content is greater the presence of carbides (NbC) or carbonitrides is inevitable and Eq. (3) loses precision. Therefore, when the steel has a composition which may give rise to the formation of complex precipitates, it is advisable to determine SRCT experimentally.

## 5. Conclusions

- (1) Static recrystallization critical temperature is always less than the solubility temperature.
- (2) Static recrystallization critical temperature depends on the strain, grain size and obviously on the content of the precipitate forming elements.
- (3) An increase in the content of any element increases the value of SRCT. Niobium in solution is the element which most contributes to increasing it.
- (4) Static recrystallization kinetics may be modelled when the temperature is below SRCT, bearing in mind the dependence of activation energy on the temperature.
- (5) Before the start of the plateau and after its finish, the recrystallization kinetics obey Avrami's law. This has made it possible to construct the model at temperatures below SRCT.
- (6) The model constructed to predict the recrystallized fraction at temperatures below SRCT does not predict the start and finish times of precipitation, as this would correspond to another model on precipitation, though it does predict the recrystallization kinetics with acceptable precision.
- (7) When the precipitates are of a complex nature, it is necessary to take care in the use of the equations which predict SRCT, it being advisable to determine SRCT experimentally.
- (8) The model constructed, together with other equations,<sup>1)</sup> may be applied in the knowledge and control of microstructures in the hot strip mill.

## Acknowledgements

The authors are grateful for the financial support of the CICYT of Spain (Projects PB89-0022 and MAT 94-0798). Mancilla's studies are sponsored by the CONACYT (Mexico).

## REFERENCES

- 1) S. F. Medina and V. López: *ISIJ Int.*, **33** (1993), 605.
- 2) S. F. Medina and J. E. Mancilla: *ISIJ Int.*, **33** (1993), 1257.
- 3) C. M. Sellars: Hot Working and Forming Processes, ed. by C. M. Sellars and G. J. Davies, Met. Soc., London, (1980), 67.
- 4) A. Le Bon, J. Rofes-Vernis and C. Rossard: *Mém. Sci. Rev. Métall.*, **57** (1973), 577.
- 5) K. J. Irvine, T. Gladman, J. Orr and F. B. Pickering: *J. Iron Steel Inst.*, **208** (1970), 717.
- 6) H. Weiss *et al.*: *J. Iron Steel Inst.*, **211** (1973), 703.
- 7) S. F. Medina and J. E. Mancilla: *Scr. Metall. Mater.*, **30** (1994), 73.
- 8) S. F. Medina and J. E. Mancilla: *Scr. Metall. Mater.*, **31** (1994), 315.
- 9) S. F. Medina, J. E. Mancilla and C. A. Hernández: *ISIJ Int.*, **34** (1994), 689.
- 10) L. N. Pussegoda and J. J. Jonas: *ISIJ Int.*, **31** (1991), 278.
- 11) F. H. Samuel, S. Yue, J. J. Jonas and B. A. Zbinden: *ISIJ Int.*, **29** (1989), 878.
- 12) F. H. Samuel, S. Yue, J. J. Jonas and K. R. Barnes: *ISIJ Int.*, **30** (1990), 216.
- 13) L. N. Pussegoda, P. D. Hodgson and J. J. Jonas: *Mater. Sci. Technol.*, **7** (1991), 129.
- 14) L. N. Pussegoda, S. Yue and J. J. Jonas: *Metall. Trans. A*, **21A** (1990), 153.

- 15) S. F. Medina and J. E. Mancilla: *ISIJ Int.*, **36** (1996), 1063.
- 16) S. F. Medina and J. E. Mancilla: *ISIJ Int.*, **36** (1996), 1070.
- 17) H. L. Andrade, M. G. Akben and J. J. Jonas: *Metall. Trans. A*, **14A** (1983), 1967.
- 18) E. T. Turkdogan: *I & SM*, (1989), May, 61.
- 19) S. F. Medina and J. E. Mancilla: *Acta Metall. Mater.*, **42** (1994), 3945.
- 20) K. Narita: *Trans. Iron Steel Inst. Jpn.*, **15** (1975), 145.
- 21) E. Hornbogen and Köster: *Recrystallization of Metallic Materials*, ed. by F. Haessner, Technische Universität Braunschweig, Germany, (1978), 159.

**Appendix**

Application of the model to calculate the recrystallized fraction corresponding to Figs. 9(a) to 9(d) and 10(a) and 10(b). Steels V2 and V3.

a) Activation energy at  $T > SRCT$

Steel V3:  $Q = 168\,632\text{ J/mol}$  .....(Ref. 15))  
 Steel V2:  $Q = 171\,470\text{ J/mol}$  .....(Ref. 15))

b) Static recrystallization critical temperature (SRCT)  
 In accordance with Eq. (2):

Steel V3:  $\epsilon = 0.35$ ;  $SRCT = 1\,234\text{ K}$   
 $\epsilon = 0.20$ ;  $SRCT = 1\,259\text{ K}$

Steel V2:  $\epsilon = 0.20$ ;  $SRCT = 1\,182\text{ K}$

c) Activation energy at  $T < SRCT$

In accordance with Eq. (5):

Steel V3:

$T = 1\,173.14\text{ K}$ ;  $\epsilon = 0.35$ ;  
 $Q^* = 1.273314 \times 10^6\text{ J/mol}$   
 $T = 1\,173.14\text{ K}$ ;  $\epsilon = 0.20$ ;  
 $Q^* = 2.760587 \times 10^6\text{ J/mol}$

Steel V2:

$T = 1\,148.14\text{ K}$ ;  $\epsilon = 0.20$ ;  
 $Q^* = 569\,197\text{ J/mol}$

d) Coefficient  $A'$

In accordance with Eq. (7):

Steel V3:

$T = 1\,173.14\text{ K}$ ;  $\epsilon = 0.35$ ;  
 $A' = 1.9563276 \times 10^{-55}\text{ s}$ ;  
 $T = 1\,173.14\text{ K}$ ;  $\epsilon = 0.20$ ;  
 $A' = 5.6299287 \times 10^{-121}\text{ s}$

Steel V2:

$T = 1\,148.14\text{ K}$ ;  $\epsilon = 0.20$ ;  
 $A' = 2.0910072 \times 10^{-24}\text{ s}$

e) Parameter  $t_{0.5}$

In accordance with Eq. (6):

Steel V3:

$T = 1\,173.14\text{ K}$ ;  $\epsilon = 0.35$ ;  $t_{0.5} = 91.4\text{ s}$ ;  
 $T = 1\,173.14\text{ K}$ ;  $\epsilon = 0.20$ ;  $t_{0.5} = 409.5\text{ s}$

Steel V2:

$T = 1\,148.14\text{ K}$ ;  $\epsilon = 0.20$ ;  $t_{0.5} = 160.1\text{ s}$

f) Recrystallized fraction ( $X_a$ )

Avrami's equation and expression of the exponent  $n$  (Ref. 16)):

$$X_a = 1 - \exp\left[-0.693\left(\frac{t}{t_{0.5}}\right)^n\right]$$

$$n = 3.07 \exp\left(-\frac{12\,000}{RT}\right)$$

Steel V3:

$T = 1\,173.14\text{ K}$ ;  $t = 2\text{ s}$ ;  $\epsilon = 0.35$ ;  $X_a = 0.02$   
 $T = 1\,173.14\text{ K}$ ;  $t = 70\text{ s}$ ;  $\epsilon = 0.35$ ;  $X_a = 0.42$   
 $T = 1\,173.14\text{ K}$ ;  $t = 10\text{ s}$ ;  $\epsilon = 0.20$ ;  $X_a = 0.03$   
 $T = 1\,173.14\text{ K}$ ;  $t = 200\text{ s}$ ;  $\epsilon = 0.20$ ;  $X_a = 0.31$

Steel V2:

$T = 1\,148.14\text{ K}$ ;  $t = 5\text{ s}$ ;  $\epsilon = 0.20$ ;  $X_a = 0.03$   
 $T = 1\,148.14\text{ K}$ ;  $t = 100\text{ s}$ ;  $\epsilon = 0.20$ ;  $X_a = 0.37$